Molecular Therapy
Nucleic Acids
Original Article

Immune tolerance promotion by LSEC-specific lentiviral vector-mediated expression of the transgene regulated by the stabilin-2 promoter

Ester Borroni,[1,4] Chiara Borsotti,[1,4] Roberta A. Cirsmaru,[1] Vakhtang Kalandadze,[1] Rosella Famà,[1] Simone Merlin,[1] Brian Brown,[2] and Antonia Follenzi[1,3]

[1]Department of Health Sciences, University of Piemonte Orientale, 28100 Novara, Italy; [2]Icahn Genomics Institute, Icahn School of Medicine at Mount Sinai, New York 10029, NY, USA; [3]Department of Attività Integrate Ricerca Innovazione, Azienda Ospedaliero-Universitaria SS. Antonio e Biagio e C.Arrigo, Alessandria, Italy

Liver sinusoidal endothelial cells (LSECs) are specialized endocytic cells that clear the body from blood-borne pathogens and waste macromolecules through scavenger receptors (SRs). Among the various SRs expressed by LSECs is stabilin-2 (STAB2), a class H SR that binds to several ligands, among which endogenous coagulation products. Given the well-established tolerogenic function of LSECs, we asked whether the STAB2 promoter (STAB2p) would enable us to achieve LSEC-specific lentiviral vector (LV)-mediated transgene expression, and whether the expression of this transgene would be maintained over the long term due to tolerance induction. Here, we show that STAB2p ensures LSEC-specific green fluorescent protein (GFP) expression by LV in the absence of a specific cytotoxic CD8$^+$ T cell immune response, even in the presence of GFP-specific CD8$^+$ T cells, confirming the robust tolerogenic function of LSECs. Finally, we show that our delivery system can partially and permanently restore FVIII activity in a mouse model of severe hemophilia A without the formation of anti-FVIII antibodies. Overall, our findings establish the suitability of STAB2p for long-term LSEC-restricted expression of therapeutic proteins, such as FVIII, or to achieve antigen-specific immune tolerance in auto-immune diseases.

INTRODUCTION

The liver is a tolerogenic organ able to not only confer tolerance to self and foreign antigens but also mount an immune response against gut-derived pathogens.[1] This has led many to propose that the hepatic compartment might be the ideal target site to obtain antigen-specific unresponsiveness when implementing therapeutic strategies that require the induction of immune tolerance to treat, among others, genetic and autoimmune disorders.[2–4] In the liver, local and systemic immune responses can be controlled not just by conventional antigen-presenting cells (APCs) but also by other non-conventional APCs, such as Kupffer cells (KCs), hepatic stellate cells, and liver sinusoidal endothelial cells (LSECs).[5] Although these highly specialized non-parenchymal cells can mount an effective adaptive immune response tailored to the hepatic environment, they are mainly known for their ability to promote tolerance. The tolerogenic function of LSECs, together with the fact that they are responsible for selective recruitment of leukocytes and activation of both naive CD4$^+$ and CD8$^+$ T cells, makes these cells the ideal site to deliver a gene of interest through viral vectors[6] or a therapeutic autoantigen encapsulated in nanoparticles.[7]

In the last decades, gene therapy has gained momentum for treating several monogenic diseases where the replacement of a missing protein, even in small quantities, can restore a healthy phenotype or, at least, ameliorate the patients' quality of life (QoL) due to its long-lasting therapeutic effect. Among single-gene diseases, hemophilia A (HA), an X-linked bleeding disorder caused by factor VIII (FVIII) deficiency or dysfunction, has attracted increasing interest as a model for gene therapy-based strategies. Indeed, to date there is still no definitive cure for HA, and current standard therapies consist of repeated administrations of recombinant or plasma-derived human FVIII, often offered as prophylaxis to patients to prevent spontaneous bleeding episodes with associated hemarthrosis.[8] In this context, a gene therapy approach able to confer long-term expression of FVIII at therapeutic levels would likely represent a highly effective treatment and, possibly, a definitive cure for HA patients, avoiding the risk of developing neutralizing antibodies (inhibitors) against FVIII.

In the last two decades, preclinical and clinical studies based on gene therapy approaches have identified adeno-associated vectors (AAVs) as effective tools to deliver the FVIII transgene[9,10] leading to their market authorization in the US (FDA Roctavian) and Europe (EMA Roctavian). Indeed, several advanced clinical studies in adult HA patients targeting FVIII expression to hepatocytes by means of a hepatocyte-specific promoter reported a therapeutic benefit following a single administration of AAV. However, both phase 1–2 and phase 3 AAV5-FVIII trials showed a gradual decrease in

Received 29 March 2023; accepted 5 January 2024;
https://doi.org/10.1016/j.omtn.2024.102116.

[4]These authors contributed equally

Correspondence: Antonia Follenzi, Department of Health Sciences, University of Piemonte Orientale, 28100 Novara, Italy.
E-mail: antonia.follenzi@med.uniupo.it

FVIII expression over time starting after the second year[11] or already after the first one,[12,13] with a constant reduction up to year 5, the longest follow-up ever reported. One of the main limitations related to the usage of AAV is the preexisting immunization to AAV capsid in about 30%–40% of the general population, which makes these patients ineligible to receive an AAV vector. In this scenario, lentiviral vectors (LVs) might be a valuable alternative for *in vivo* delivery of therapeutic genes due to their ability to integrate their DNA into the host genome, the size available for the expression cassette and the low prevalence of HIV infection in humans.[14]

FVIII has been shown to be largely synthetized and secreted by endothelial cells (ECs), more specifically by LSECs, rather than by hepatocytes.[15–18] In particular, our group has recently reported that the injection of LVs carrying the FVIII transgene under the control of endothelial-specific promoters (i.e., the VE-cadherin [VEC, known as cadherin 5 CDH5] promoter) in HA mice results in efficient long-term cell-type-specific FVIII expression and activity without inhibitor development.[19] While the VEC promoter was effective at achieving stable FVIII activity, because the promoter is pan-endothelial, expression was not confined to LSECs, and thus secretion of FVIII was not confined to the more tolerogenic context of the liver. Thus, we sought to develop a vector with LSEC-restricted expression. Gene expression analysis of LSECs has previously identified the *stabilin-2* (*STAB2*) gene as being uniquely expressed in LSECs.[20] STAB2 is a type I membrane protein belonging to class H scavenger receptors (SRs) involved in binding, uptake, and degradation of multiple ligands, such as hyaluronic acid,[21] phosphatidylserine, heparin, and von Willebrand factor-FVIII complex.[17,22] Thus, here we asked whether the STAB2 promoter (STAB2p) could be used *in vivo* to direct specific transgene expression in LSECs following LV transgene delivery, and whether that would ensure a stable expression of the protein due to tolerance induction. To this end, we employed two different LV constructs: one carrying the green fluorescent protein (GFP), which allowed us to analyze cell-type-specific expression of the transgene and verify the induction of immune tolerance to the xenogeneic protein, and the other one driving the expression of ectopic FVIII, which enabled us to assess the therapeutic correction of the hemophilic phenotype.

RESULTS

Endothelial-specific activity of the STAB2 promoter *in vivo*

First, to test the endothelial-specific activity of several promoters, we investigated the activity of stabilin-1 and -2 promoters. In initial *in vivo* experiments we found that the STAB1 promoter was active in hepatocytes, macrophages, and sinusoidal ECs (Figure S1) while STAB2 was mainly active in LSECs. Then, we injected an LV expressing the reporter gene GFP under the control of STAB2p (LV.STAB2-GFP) in the tail veins of C57BL/6 or BALB/c mice. Two weeks or 1 month after LV injection, GFP expression was preferentially displayed in endothelial lymphatic vessel endothelial hyaluronan receptor 1 (LYVE1)-positive cells in the liver of C57BL/6 mice (Figures 1A–1F, S2A, and S2B), with no difference between the two time points and with small off-target signals in other hepatic cell types, such as F4/80$^+$ KCs (Figures 1G–1L, 1M, and 1N). By contrast, the expression of GFP driven by the ubiquitous PGK promoter was evident up to 1 month in all the main hepatic cell populations: hepatocytes, ECs, and F4/80$^+$ KCs (Figures S3A–S3F and S3M), thus confirming the endothelial specificity of STAB2p. C57BL/6 mice are more tolerant to introduction of GFP, whereas BALB/c mice rapidly develop a very strong immune response to GFP.[23] Indeed, when BALB/c mice were injected with LV.PGK-GFP, we observed the complete clearance of GFP$^+$ cells 2 weeks after injection (Figures S3G–S3L and S3N). In striking contrast, when mice were injected with LV.STAB2-GFP, GFP was visible at early time points (Figures 2A–2F, S2C–S2E, and 3A–3F) and was maintained up to 3 months post-injection (Figures 2G–2L, S2F, and3G–3L). This indicates that STAB2p-driven expression in LSECs is able to prevent immune clearance of transgene-expressing cells. Even though we observed few off-target GFP$^+$ hepatocytes, most green cells were LSECs, as judged by their morphology and LYVE1 positivity. Quantification of red/green immunofluorescence (IF) overlapping confirmed the LYVE1-restricted GFP expression at all time points (Figures 3M–3P). In addition, the spleens of LV.STAB2-GFP-injected mice showed only few GFP-expressing cells mainly located around the germinal centers (GCs) (Figures S4 and S5), whose morphology resembled that of the ECs lining the sinus of the GC.[24] These GFP$^+$ cells were not macrophages as shown by the absence of co-staining with F4/80 (Figures S5S–S5U). Finally, we analyzed by flow cytometry the main immune cell populations in both C57BL/6 and BALB/c mice 2 weeks after LV delivery. Interestingly, the percentage of hepatic CD8$^+$ T cells was increased significantly in LV.STAB2-GFP- vs. LV.PGK-GFP-injected BALB/c mice (Figure S6B). A similar trend was observed in C57BL/6 mice as well (Figure S6A). The percentage of splenic CD8$^+$ T cells was not differentially affected by LV injection, while the percentage of CD19$^+$ B cells and CD11b$^+$ myeloid cells was slightly increased in LV.STAB2-GFP-treated BALB/c mice (Figures S6C and S6D). Overall, these data indicate that STAB2p confers LSEC-specific gene expression by LV in the absence of a specific immune reaction against transgene-expressing cells.

STAB2p-driven GFP expression prevents an antigen-specific cytotoxic CD8 T cell immune reaction *in vivo*

To ascertain the role of STAB2p in modulating the immune response in the liver of LV-injected mice, we employed Just EGFP death-inducing (JEDI) mice, which carry CD8$^+$ T cells that have a T cell receptor that recognizes the immunodominant epitope of GFP ($GFP_{200-208}$) presented on MHC class I.[25] Initially, B10.D2 mice, which are syngeneic with JEDI mice, were injected with LV.STAB2-GFP, LV.VEC-GFP—used to target ECs[19]—or LV.PGK-GFP. Ten days after LV administration, we checked the GFP expression in the liver sections of the mice and found that the samples obtained from all the LV-injected animals displayed GFP$^+$ cells (Figure S7). We repeated the experiment adoptively transferring the mice with 1.5–2 $\times$ 10^6 splenic CD8$^+$ T cells isolated from either JEDI or B10.D2 mice 10 days after the LV injection (Figure 4A). After 4 days, we collected tissues and analyzed GFP expression. In mice injected with LV.STAB2-GFP, GFP was readily visible in the liver of all animals, including the cohort that received the GFP-specific JEDI CD8$^+$ T cells (Figures 4H–4J). GFP$^+$ cells showed a characteristic

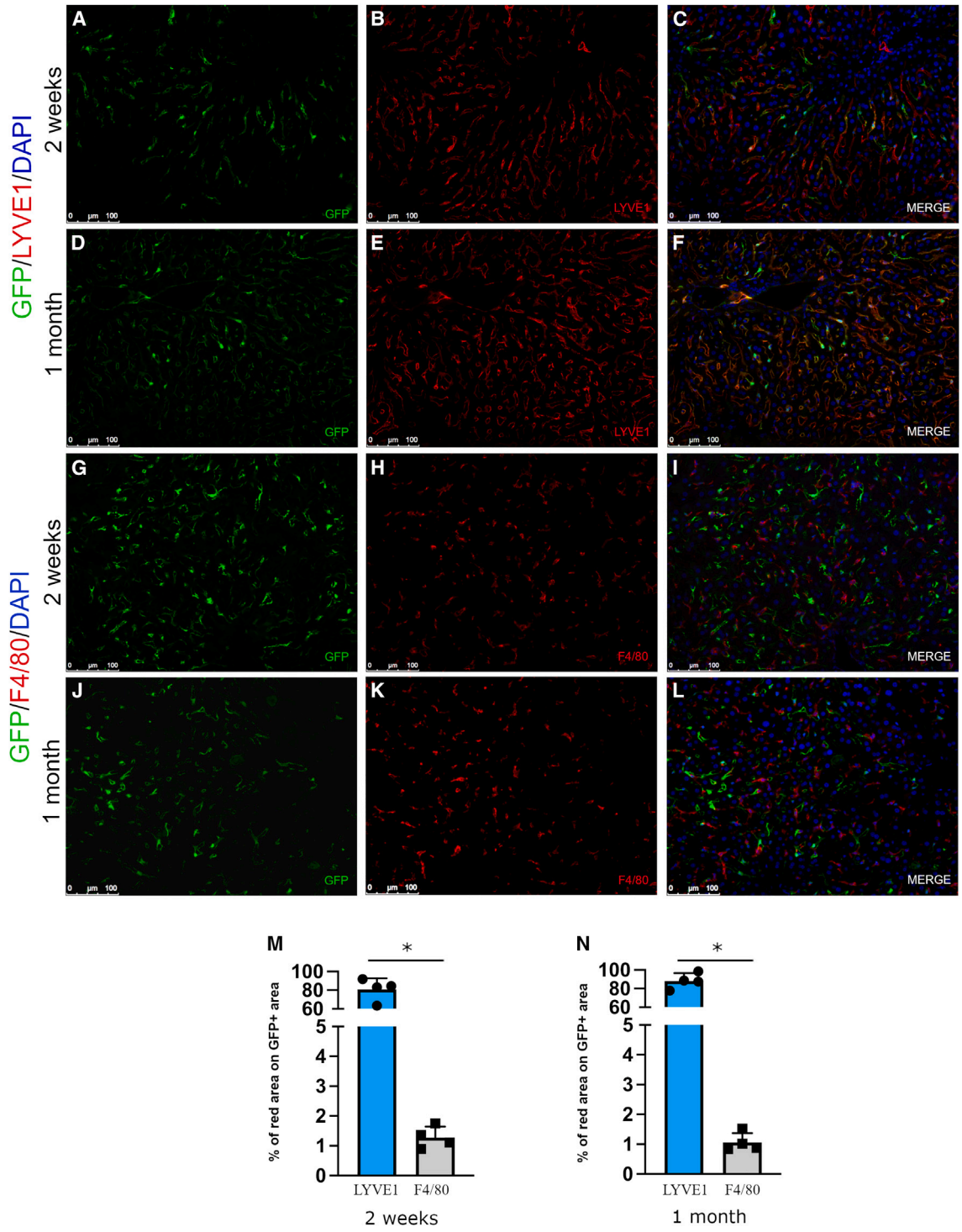

Figure 1. Hepatic expression of GFP after delivery of LV.STAB2-GFP in C57BL/6 mice

C57BL/6 (n = 8) mice were injected with 5×10^8 TU of LV.STAB2-GFP, and 2 weeks or 1 month later GFP expression in liver sections was evaluated by immunofluorescence using antibodies against GFP and LYVE1 as endothelial marker (A–F) or against GFP and F4/80 as macrophage marker (G–L). Scale bars, 100 μm. Green, GFP; red, LYVE1 or F4/80; nuclei were stained in blue (DAPI). Percentage of red area extension (LYVE1 or F4/80) over total GFP area at (M) 2 weeks and (N) 1 month (single dots represent an average of six IF images quantified per mouse, error bars represent SD) (*$p < 0.05$).

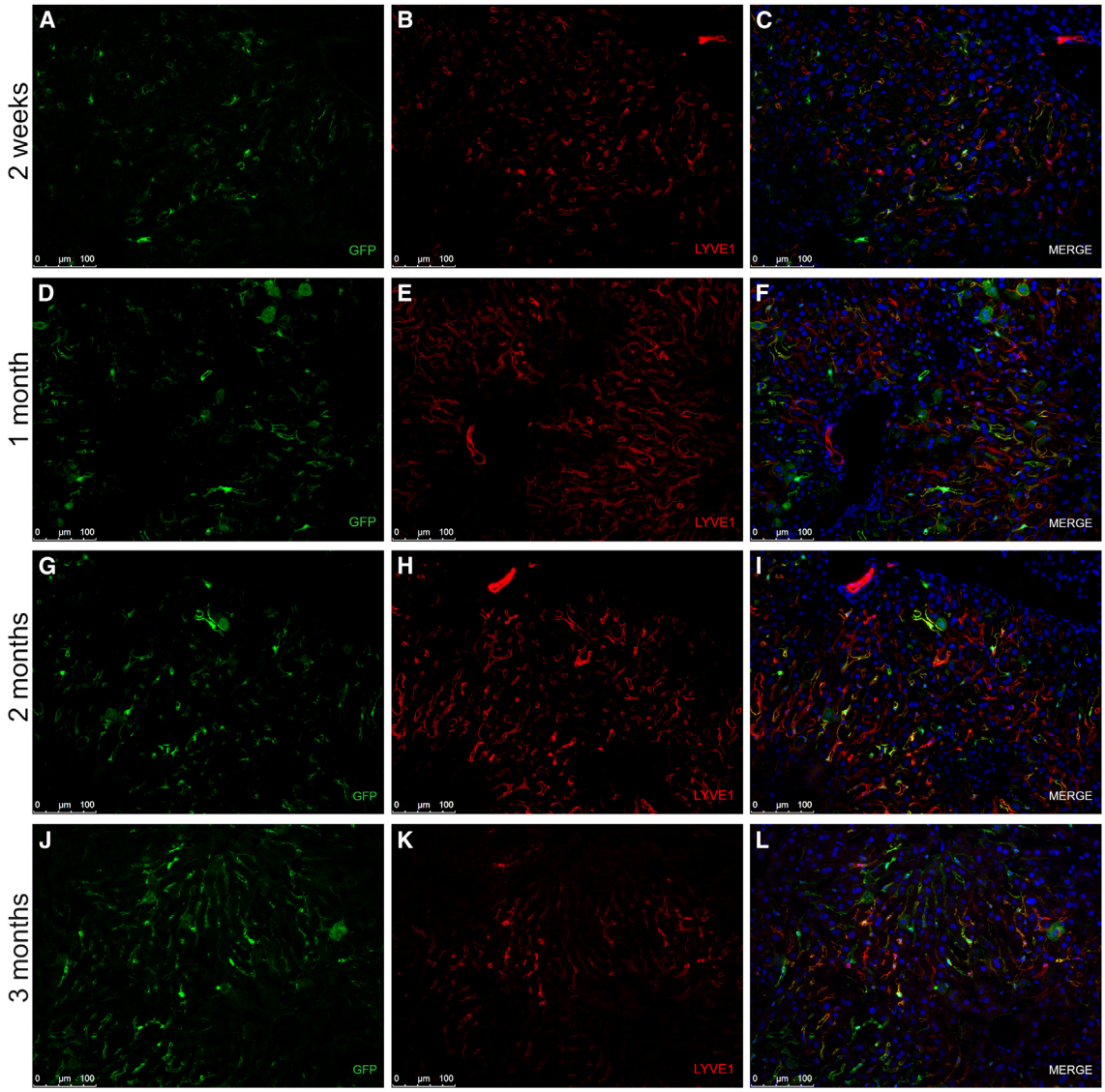

Figure 2. Hepatic expression of GFP after delivery of LV.STAB2-GFP in BALB/c mice

BALB/c (n = 16) mice were injected with 5×10^8 TU of LV.STAB2-GFP and GFP expression in liver sections was assessed by immunofluorescence at different time points: (A–C) 2 weeks, (D–F) 1 month, (G–I) 2 months, and (J–L) 3 months. Scale bars, 100 µm. Green, GFP; red, LYVE1; nuclei were stained in blue (DAPI).

endothelial morphology even in mice receiving JEDI $CD8^+$ T cells (Figure 4J). In contrast, GFP expression was completely absent in any mice injected with LV.PGK-GFP (Figures 4E–4G) or LV.VEC-GFP (Figures 4K–4M), indicating a strong reaction of the host immune system (Figures 4E and 4K) independently of the transferred $CD8^+$ T cells. Indeed, all the hepatic sections displayed hypercellularity, as demonstrated by the high number of nuclei due to enhanced cell recruitment, and by the presence of activated $F4/80^+$ KCs, probably involved in the clearance of GFP-expressing cells. Quantification of GFP^+ area confirmed the presence of GFP^+ cells only in the mice injected with LV.STAB2-GFP (Figure 4N). To investigate if the strong immune response in the LV.VEC-GFP-injected mice was due to the occasional off-target GFP expression, we repeated the CD8 T cell adoptive transfer in mice previously injected with the same vector carrying the combination of microRNA target sequence (miRTs) 122.142. These two sequences are able to prevent the expression of the transgene in hepatocytes and hematopoietic cells, respectively.[19] However, a strong immune response was still detectable in the LV.VEC-GFP.122.142 mice, which displayed a complete clearance of GFP^+ cells (Figures S8A–S8C). Altogether, these results confirm that *in vivo* GFP expression driven by STAB2p in LSECs is able to abolish a strong immune reaction even in the presence of a high number of GFP-specific T cells, indicating that LSEC-driven expression can mediate robust tolerance to a transgene-derived antigen.

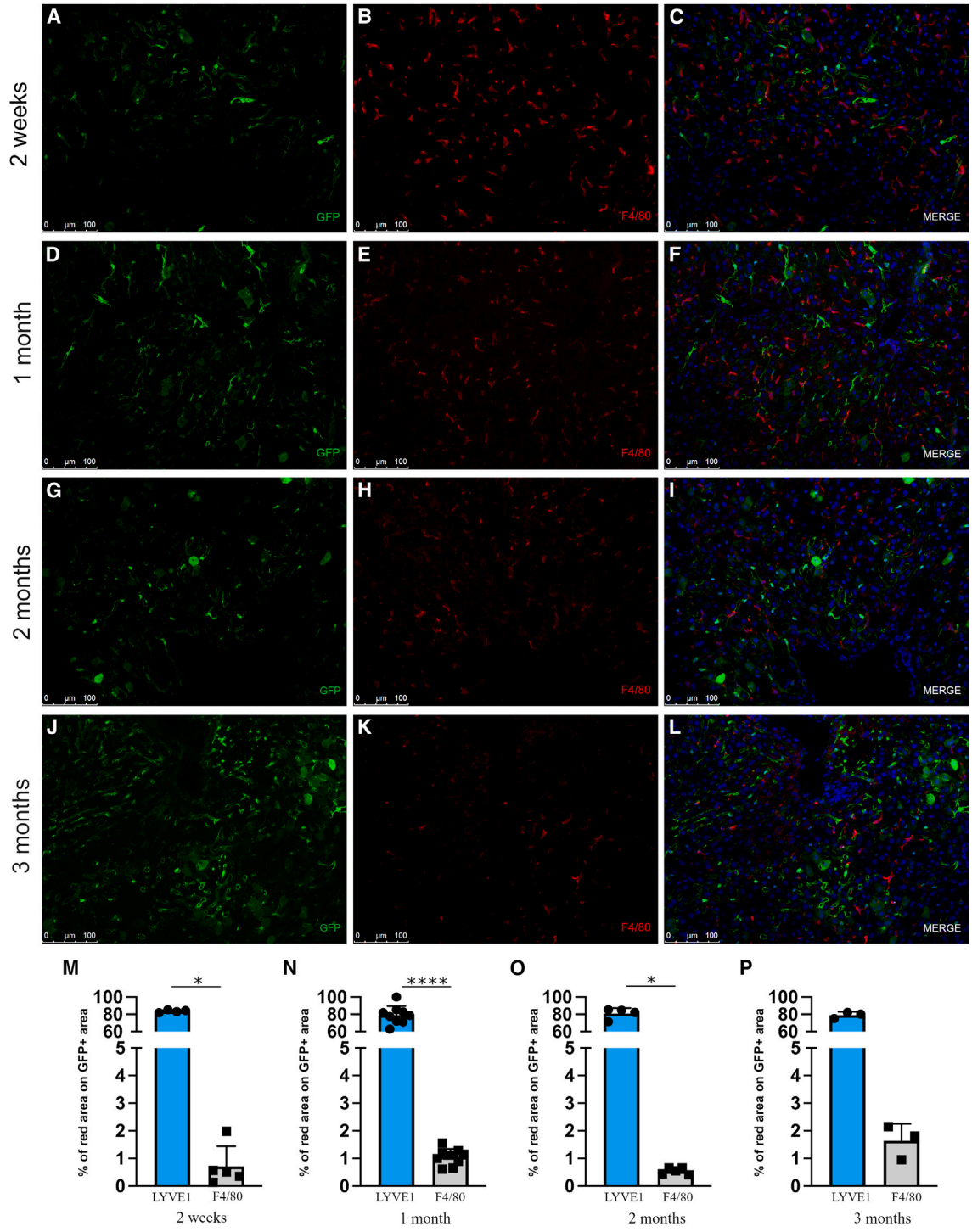

Figure 3. Absence of GFP⁺ macrophages after *in vivo* delivery of LV.STAB2-GFP in BALB/c mice

BALB/c (n = 16) mice were injected with 5×10^8 TU of LV.STAB2-GFP and GFP expression in liver sections was assessed by immunofluorescence at different time points: (A–C) 2 weeks, (D–F) 1 month, (G–I) 2 months, and (J–L) 3 months. Scale bars, 100 µm. Green, GFP; red, F4/80; nuclei were stained in blue (DAPI). Percentage of red area extension (LYVE1 or F4/80) over total GFP area at (M) 2 weeks, (N) 1 month, (O) 2 months, and (P) 3 months (single dots represent an average of 6 IF images quantified per mouse, error bars represent SD) (*$p < 0.05$, ****$p < 0.0001$).

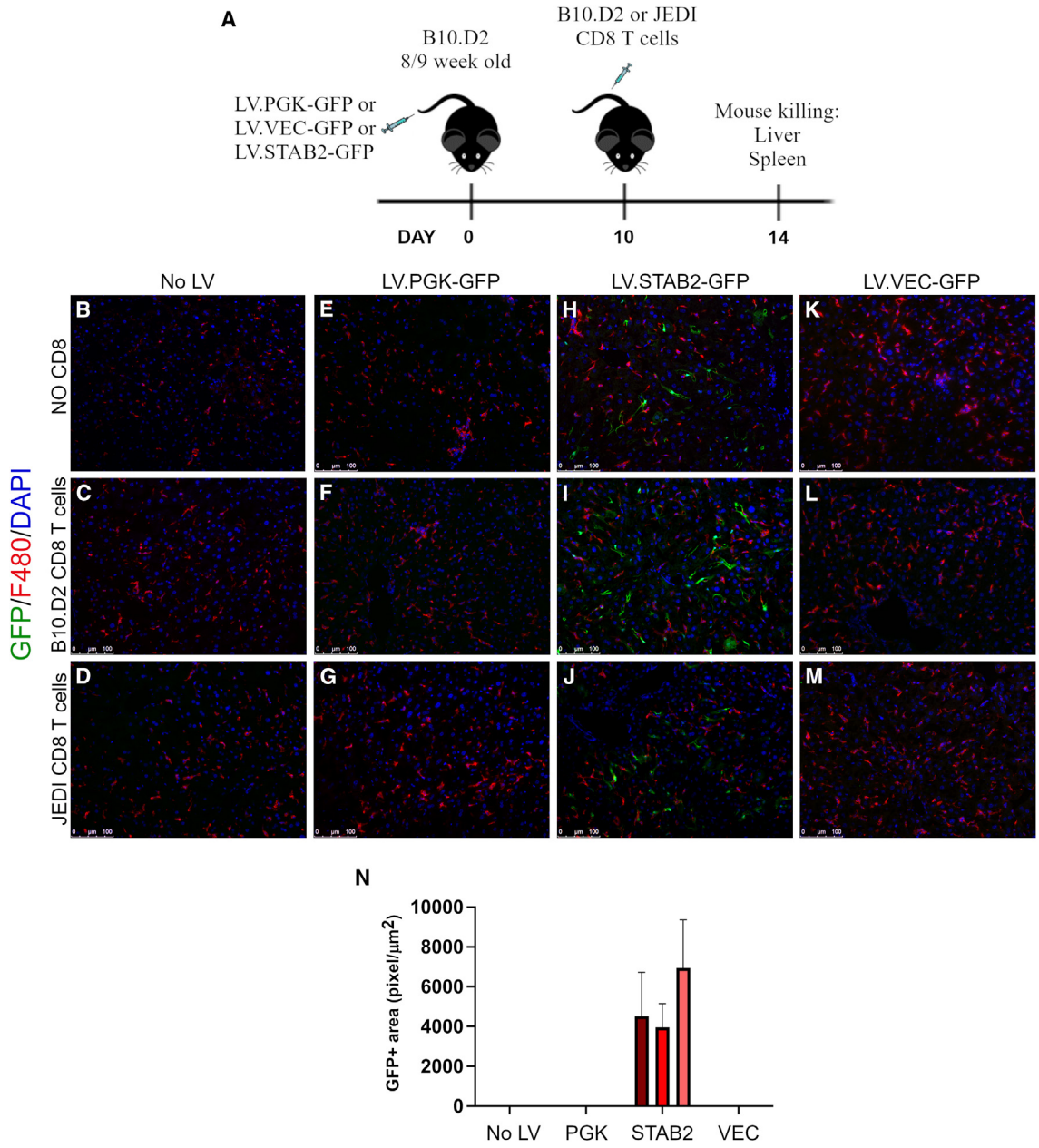

Figure 4. GFP expression after adoptive transfer of CD8⁺ T cells in B10.D2 mice following LV delivery

(A) Schematic representation of the experimental plan. B10.D2 mice were injected with 3×10^8 TU of LV.PGK-GFP (n = 19) or 5×10^8 TU of LV.VEC-GFP (n = 14) or LV.STAB2-GFP (n = 27). Ten days later, 1.5–2 $\times$ 10^6 $CD8^+$ T cells isolated from either B10.D2 or JEDI mice were transferred to mice. Four days after the transfer (in total 14 days from LV delivery), the recipient mice were killed, and their livers were processed for GFP assessment by immunofluorescence. (B–D) Liver sections from control mice: (B) untreated, (C) receiving $CD8^+$ T cells from B10.D2, or (D) receiving $CD8^+$ T cells from JEDI mice. (E–G) Mice receiving LV carrying the ubiquitous PGK promoter. (H–J) Mice receiving LV carrying the STAB2 promoter. (K–M) Mice receiving LV carrying the VEC promoter. Scale bars, 100 µm. Green, GFP; red, F4/80; nuclei were stained in blue (DAPI). (N) Quantification of GFP^+ area expressed as pixels/μm^2 (n = 5–8 mice, 6 images per mouse, error bars represent SD).

PD1 upregulation on hepatic CD8 T cells upon LV injection

To further characterize the main immune cell populations present in the challenged mice, we calculated their relative percentages in the liver and spleen by flow cytometry 14 days after LV delivery (Figure 5). All LV-injected mice displayed a higher percentage of $CD8^+$ T cells compared with non-injected B10.D2 (Figures 5A–5D), especially those that had received $CD8^+$ T cells (Figures 5C and 5D). The highest $CD8^+$ T cell percentage was seen in LV.PGK-GFP-injected mice

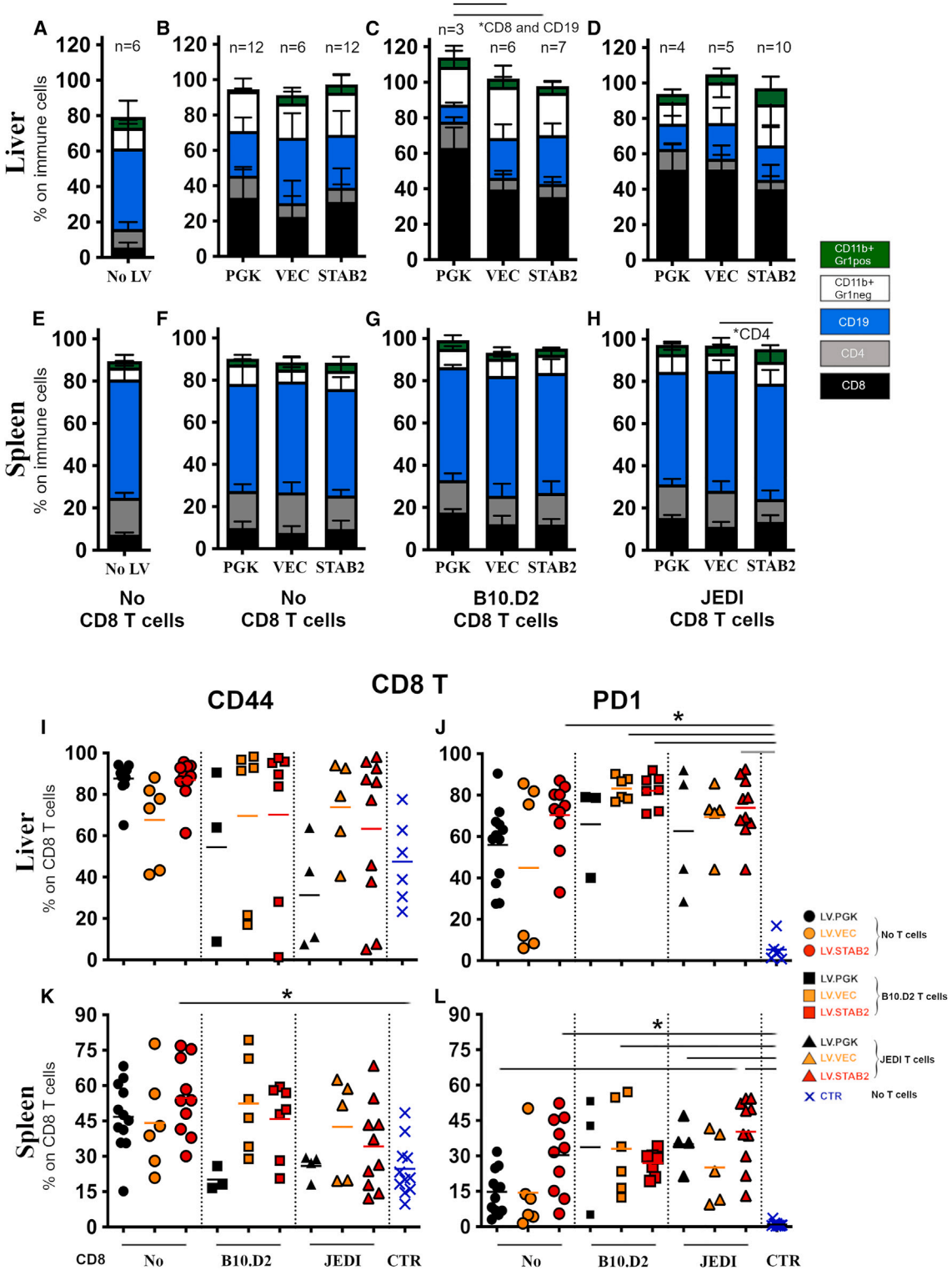

Figure 5. Immune cell population analysis after CD8 T cell adoptive transfer in B10.D2 mice injected with different LVs

Four days after CD8 T cell adoptive transfer, mice were killed and hepatic and splenic leukocytes were analyzed by flow cytometry after Ficoll-Paque gradient centrifugation or red blood cell lysis, respectively. (A and E) Non-injected mice (n = 5) were used as control. (B–D) Immune cells analysis of mouse livers after receiving only LV (B), B10.D2 CD8

(legend continued on next page)

receiving B10.D2 CD8$^+$ T cells (Figure 5C). Nevertheless, we detected CD8$^+$ T cells recruited to the liver upon LV challenge also in mice still showing GFP$^+$ cells at the same time point, indicating that they were able to sense the transduced cells even in the absence of a significant immune response. Conversely, the relative composition of splenic immune cells was not altered by LV injection (Figures 5E–5H), probably due to the low GFP expression levels observed in that organ.

To better understand the activation state of the CD8$^+$ T cells found in the liver and spleen, we analyzed the expression of two markers: CD44, known to be present on the surface of T cells exposed to an antigen, and programmed cell death 1 (PD1), an inhibitory regulator of T cell activity upregulated in response to TCR-mediated activation and downregulated following antigen clearance.[26] The expression of PD1$^+$ on CD8$^+$ T cells was greatly increased in LV-injected mice compared with that of non-injected mice, reaching at least 60% in the liver (Figure 5J) and 15% in the spleen (Figure 5L). Of note, all the mice injected with LV.STAB2-GFP showed statistically higher expression of PD1 on CD8$^+$ T cells than the control mice. In contrast, we observed only a slight increase in the CD44 percentage on CD8$^+$ T cells in the livers (Figure 5I) and spleens (Figure 5K) of animals similarly injected. Due to the high variability within several single experimental groups, we did not observe any statistical differences between mice receiving the different LVs. Interestingly, the analysis of the same two markers on CD4$^+$ T cells did not reveal any difference in the percentage of CD44$^+$ cells (Figures S9A and S9C), while the percentage of PD1$^+$ cells was higher than that observed in non-injected mice only in LV.PGK-GFP-injected animals receiving additional CD8$^+$ T cells (Figure S9B).

Overall, the aforementioned results indicate a general hepatic recruitment and priming of CD8$^+$ T cells sensing GFP expression in response to LV injection. The subsequent different immunoreactivity appears to be modulated by the various cell types presenting the GFP epitopes, with LSECs—specifically targeted by STAB2p—being able to induce tolerance rather than cytotoxicity. Conversely, KCs seem to act as main GFP APCs in mice injected with LV.PGK-GFP, triggering CD8$^+$ T cell killing activity.

To further verify that the injection of LV.STAB2-GFP was able to inhibit the cell immune reaction against GFP-expressing cells, we co-cultured for 3 days GFP$^+$ peritoneal macrophages with leukocytes obtained from B10.D2 mice previously injected with LV.PGK-GFP or LV.STAB2-GFP (Figure S10A). Splenocytes from non-injected B10.D2 and from JEDI mice were used as negative and positive controls, respectively. While the percentage of viable GFP$^+$ macrophages shrank by half in the presence of splenocytes from LV.PGK-GFP- vs. LV.STAB2-GFP-injected mice (Figure S10C), the number of CD8$^+$ T cells recovered in each well and the quantity of Granzyme B secreted after 3 days of co-culture with GFP$^+$ macrophages were lower in LV.STAB2-GFP than in LV.PGK-GFP splenocytes (Figures S10E and S10G). Altogether, these *in vitro* data suggest that CD8$^+$ T cells *in vivo* primed by LSECs targeted by LV.STAB2-GFP were less reactive toward GFP$^+$ macrophages.

Long-term and stable correction of the hemophilic phenotype by LV.STAB2-FVIII injection into HA mice

Based on the aforementioned results, we next sought to determine the feasibility and efficacy of STAB2p-driven expression of FVIII in hemophilic mice. Specifically, we asked whether our strategy would allow establishing a physiological expression of FVIII without eliciting an adverse immune response against this protein. To assess the correction of the bleeding phenotype, we injected C57BL/6 HA mice with the LV.STAB2-FVIII-B-domain deleted (BDD) or LV.STAB2-FVIII-RH constructs, both expressing functional FVIII proteins, albeit with different therapeutic strengths,[19] and periodically measured FVIII activity and levels of FVIII-specific antibodies for up to 48 weeks by activated partial thromboplastin time (aPTT) and ELISA, respectively. We observed partial correction of FVIII activity (10%) by both LVs as early as 2 weeks from injection, which remained between 10% and 14%, respectively, for the entire duration of the experiment (Figures 6A and 6B). Importantly, we did not detect the appearance of anti-FVIII IgG antibodies (Figures 6C and 6D). Similarly, FVIII activity (Figure S11A) increased quickly after LV delivery with no anti-FVIII IgG antibody formation (Figure S11B) in a different immunocompetent hemophilic mouse strain, namely B6/129. Of note, the LV.STAB2-FVIII-RH construct showed a significantly higher FVIII activity over time compared with the LV.STAB2-FVIII-BDD (14% vs. 10%). Finally, blood loss assay after clip challenge confirmed the therapeutic restoration of FVIII activity since both HA mice strains receiving the LV carrying the FVIII behaved similarly to C57BL/6 wild-type mice (Figure S11C).

Given that STAB2p drives FVIII expression in LSECs, and that these latter are known to promote tolerance by interacting with T regulatory cells (Tregs),[27] we sought to determine whether LSEC-induced Tregs would play a role in FVIII tolerance induction. For this purpose, we depleted Tregs by administering a single injection of α-CD25 either 14 weeks after or 5 days before LV.STAB2-FVIII delivery. In the first case, both LV.STAB2-FVIII- and LV.STAB2-FVIII RH-injected C57BL/6 HA mice quickly acquired a stable percentage of FVIII activity. However, after 2 weeks, FVIII activity started to decrease, reaching its lowest value (50%–60% of reduction) 14 weeks after Treg depletion, corresponding to 28 weeks after the LV injection (Figures 6A and 6B). Fittingly, anti-FVIII IgG antibodies began to increase, peaking at the same time point of the lowest FVIII activity (Figures 6C and 6D) and disappeared over time, concomitantly with the restoration of FVIII activity. Conversely, FVIII activity was

T cells (C), or JEDI CD8 T cells (D). (F–H) Immune cells analysis of mouse spleens after receiving only LV (F), B10.D2 CD8 T cells (G), or JEDI CD8 T cells (H). Statistical analysis was performed by two-way ANOVA with Tukey's multiple comparison test (****$p < 0.0001$ in C or *$p < 0.05$ in H); error bars represent SD. (I) Collected hepatic CD8 T cells were analyzed for CD44 and (J) PD1 expression. (K) Collected splenic CD8 T cells were analyzed for CD44 and (L) PD1 expression. Statistical analysis was performed by Kruskal-Wallis test with Dunn's multiple comparison test (*$p < 0.05$, **$p < 0.005$, ****$p < 0.0001$).

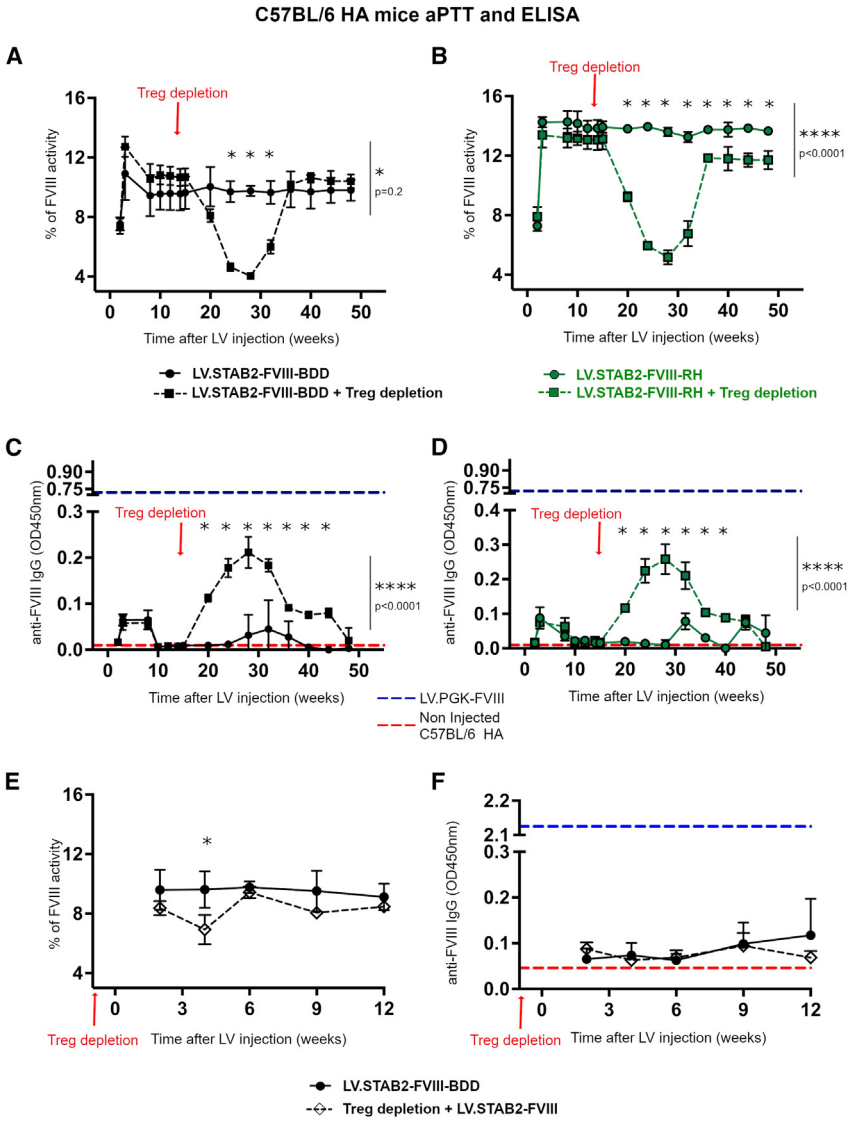

Figure 6. Assessment of FVIII activity and anti-FVIII IgG formation in C57BL/6 HA mice after injection of LV.STAB2-FVIII

C57BL/6 mice were intravenously injected with 10^9 TU of LV.STAB2-FVIII or LV.STAB2-FVIII-RH. A group of mice was Treg depleted after 14 weeks (n = 4) while, in a separate experiment, a group of mice was Treg depleted 5 days before (n = 6) the LV injection. Mouse plasma was regularly collected and assessed for FVIII activity by aPTT and for the presence of anti-FVIII IgG by ELISA (plasma samples diluted 1:200). (A) LV.STAB2-FVIII (n = 8) and (B) and LV.STAB2-FVIII-RH (n = 8) injected in C57BL/6 HA mice. (C and D) Specific anti-FVIII IgG were detected in the plasma of LV.STAB2-FVIII and LV.STAB2-FVIII-RH C57BL/6 mice only after the Treg depletion. Comparison of FVIII activity (E) and specific anti-FVIII IgG level (F) in plasma of control (n = 4–13) vs. Treg depleted (n = 4–6) C57BL/6 HA mice. Statistical analysis was performed by two-way ANOVA with Sidak's multiple comparison test (*p < 0.05, ****p < 0.0001); error bars represent SD. Dashed red line represents a non-injected C57BL/6 HA mouse (negative control), while the dashed blue lines represent a C57BL/6 HA mouse injected with LV.PGK-FVIII (positive control).

only slightly diminished by the Treg depletion carried out 5 days prior to the LV administration (Figure 6E). Indeed, from week 6 FVIII activity was similar between control and Treg-depleted animals. Accordingly, no specific α-FVIII IgG was detected in their plasma samples (Figure 6F).

Taken altogether, these data obtained in a pre-clinical model of HA confirm that endothelial-specific expression driven by STAB2p leads to stable FVIII secretion and activity without formation of anti-FVIII antibodies in two different immunocompetent HA mouse strains. Moreover, Tregs are involved in the establishment and maintenance of tolerance toward FVIII.

DISCUSSION

LSECs line the liver sinusoids where the relative low blood flow allows these cells to interact with circulating lymphocytes and injected LVs. Indeed, murine LSECs are more efficient than KCs in the uptake and elimination of HIV-like particles,[28] and they can induce *in vitro* and *in vivo* $CD8^+$ T cell tolerance rather than a cytotoxic response[29,30] by promoting the conversion of effector $CD8^+$ T cells to memory $CD8^+$ T cells, which are unresponsive under steady-state conditions.[31,32] Similarly, the interaction between LSECs and $CD4^+$ T cells results in the inhibition of inflammatory responses[33,34] and peripheral Treg differentiation due to their ability to retain TGF-β on the cell surface.[2]

Here, we investigated *in vivo* the role of LSECs in establishing immune tolerance toward xenogeneic proteins such as GFP and FVIII, with the latter being more clinically relevant. To this end, we specifically targeted LSECs by using LVs carrying the desired transgene under the control of STAB2p. The specificity of this promoter was confirmed by liver IF of all the three mouse strains injected with the LV.STAB2-GFP construct (i.e., C57BL/6, BALB/c, and B10.D2), which evidenced the endothelial morphology of all GFP^+ cells, which were also co-stained by an antibody against the LYVE1 protein, a marker shared by LSECs and lymphatic endothelial cells.[35] A quick and strong immune reaction was observed in the liver when GFP expression was driven by the ubiquitous PGK promoter in BALB/c and B10.D2 mice, indicating that the transduced macrophages in the liver and spleen were acting as APCs, thus triggering the cytotoxic activity of $CD8^+$ T cells.

Innate immune responses to LV particles and genomic RNA can easily contribute to the generation of a proinflammatory environment recruiting the adaptive immune arm,[36] thus leading to the rejection of transgene-expressing cells. Strikingly, our LSEC-targeted expression system in immune-reactive mouse strains allowed us to maintain the expression of GFP over the long term. Tolerization to transgene-expressing cells was observed even when GFP-specific JEDI $CD8^+$ T cells were adoptively transferred in LV.STAB2-GFP-injected mice, whereas GFP^+ cells were eliminated from the liver in all LV.PGK-GFP-injected B10.D2 mice regardless of the type of injected $CD8^+$ T cells. Furthermore, these mice displayed a robust hepatic inflammation, as judged by the presence of tissue hypercellularity and KCs characterized by many elongated cytoplasmic processes. A similarly strong immune reaction was evident in LV.VEC-GFP-injected B10.D2 mice, even in presence of the miRTs-122.142 sequence, thus suggesting that the transgene expression in other ECs other than LSECs may play an important role and trigger the immune response. While STAB2 expression in the liver is confined in the sinusoids, it can also be detected in the medullary sinuses of lymph nodes and splenic sinusoids.[37] However, in our *in vivo* models we did not observe many GFP^+ cells in the latter organs after LV.STAB2-GFP injections, suggesting that LSECs are the ECs playing the major role in establishing specific tolerance. We previously reported that the use of the VEC promoter with or without the miRTs-122.142 sequence was able to favor tolerance toward the GFP protein in C57BL/6 mice,[19] which has been shown to be less immuno-reactive even when the expression of the transgene was regulated by the PGK promoter. Instead, the B10.D2 mice employed here for the CD8 T cell adoptive transfer experiments were strongly rejecting the cells expressing the GFP in all LV-injected mice except the ones receiving LV.STAB2-GFP. These results confirm the goodness of the STAB2p in achieving the transgene tolerance even in more vulnerable settings (e.g., autoimmune conditions).

LSEC-primed $CD8^+$ T cells have been reported to expand and acquire a memory and a hyporesponsive phenotype due to the absence of co-stimulatory molecules on the LSEC surface and to the involvement of the PD-L1/PD1 axis.[38,39] Recruitment of $CD8^+$ T cells in the liver was consistent in all LV-injected mice, independent of tolerance generation. As LSECs express MHC class I, transduced LSECs can present directly GFP peptides to both endogenous and administered $CD8^+$ T cells. PD1 expression was substantially upregulated in $CD8^+$ T cells obtained from the livers of LV-treated mice and its expression levels did not correlate with the acquisition of tolerance induction. We performed flow cytometry analysis 2 weeks after the LV injections, when the acute cellular rejection phase was over and therefore most of the effector cytotoxic $CD8^+$ T cells should already have undergone the contraction phase and thus eliminated,[40] leaving mainly resting or exhausted lymphocytes. The partial tolerization of LSEC-primed $CD8^+$ T cells generated *in vivo* by LV.STAB2-GFP injection was further confirmed by the observation that LV.STAB2-GFP $CD8^+$ T cells were less cytotoxic than their LV.PGK-GFP-injected counterparts when co-cultured *in vitro* with GFP^+ macrophages.

The long-term safety and stability of LV-mediated targeting of LSECs was investigated by injecting LVs carrying the human FVIII gene under the control of STAB2p in HA mice. A quick and long-term partial restoration of FVIII activity was observed in both hemophilic mouse strains tested, ranging from 8% to 14%, values enough to reduce the risk of spontaneous bleeding in patients and to improve their QoL.[41] Notably, these levels were even above the ones we reported previously when we injected the same mice with LV carrying FVIII (BDD or RH form) under the control of the endothelial VEC promoter[19] or the F8 native promoter.[42] The maintenance over time of the therapeutic FVIII activity was accompanied by the absence of specific anti-FVIII IgG development, further corroborating the tolerogenic role played by LSECs. Of note, in this case the avoided immune response was directed against a secreted protein, FVIII, which has been shown to be highly immunogenic in HA patients[43] and is xenogeneic in our experimental setting (human FVIII produced in mice). Even though direct inhibition of B cells by LSECs has not been reported, their humoral-specific response might be prevented through their well-documented ability to inhibit $CD4^+$ T cell differentiation in Th1 and Th17 effectors[34] and to promote Treg differentiation.[2] Without the proper $CD4^+$ T cell help, FVIII-specific B cells would not be able to mature in antibody-secreting cells. More importantly, LV.STAB2-FVIII-transduced LSECs might stimulate the formation of FVIII-specific Tregs, able to block the activation of both $CD8^+$ T and B cells. The role of Tregs in the *in vivo* maintenance of FVIII tolerance was supported by the appearance of anti-FVIII IgG in HA mice depleted of Tregs after the LV.STAB2-FVIII injection. Interestingly, the depletion of Treg before the LV administration lightly and briefly affected the percentage of FVIII activity, suggesting that there could be other immunological mechanisms (e.g., clonal deletion, anergy) participating in establishing FVIII tolerance in synergy with the Treg activity. Moreover, the majority of the Tregs involved in the FVIII tolerance might be induced (i)Tregs, generated by the interaction between the LSECs and circulating naive CD4 T cells, rather than natural (n)Tregs developed in the thymus.[44] It is intriguing to speculate that, when the α-CD25 antibody is given long after the vector injection, once the tolerance is already established, the depletion eliminates all the circulating FVIII-specific iTregs previously generated, causing a quick drop of FVIII activity and increase in antibody level. Instead, Treg depletion prior to LV administration affects nTregs but does not alter the first presentation by the transduced LSECs of the FVIII-derived peptide to the naive CD4 T cells, promoting their possible differentiation in new FVIII-specific iTregs. Besides the prevention of inhibitor formation, the capability of LSECs to tolerize $CD8^+$ T cells against FVIII-transduced cells might be a further advantage in the application of gene therapy approaches for HA treatment, since the ongoing clinical trials have so far been unable to demonstrate the absence of cytotoxic immune response over the long term due to the limited follow-up of those studies.[45]

In conclusion, our data show the feasibility and efficacy to target LSECs for the development of new gene transfer applications, especially when an immunomodulation is required, either toward an autoimmune antigen or a therapeutic product since both humoral

and cellular responses are suppressed. The translatability of these results in clinical settings would require further studies in larger animal models, such as hemophilic dogs, to confirm the safety and efficacy of this gene therapy approach over a long period of time. One challenge might be represented by the difficulty of obtaining tolerance toward the transgene therapeutic protein once the autoimmunity has already been established, since the immune mechanisms involved in the eradication of pre-existing auto-antibodies and specific cytotoxic T cells are different from the ones active in the tolerance formation at the time of the first encounter with the auto-antigens.

MATERIAL AND METHODS

Plasmids and LV production

The STAB2p (1,238 bp) and STAB1 promoter (1,250 bp) were obtained by PCR amplification of the proximal region of the regulated gene from human genomic DNA using the following primers: (Fw) 5′- cttcctcgagcgtttccatcatggtttc-3′ and (Rv) 5′-cttcaccggtgaggaaatatttgctccttctc-3′ for STAB2p and (Fw) 5′- cttcctcgaggccacctccattcatttattc-3′ and (Rv) 5′-cttcaccggtgggcggcctgagccctgctc-3′ for STAB1 and subcloned into the LV construct carrying GFP through the restriction enzymes XhoI and AgeI. LV.STAB2-FVIII, either the BDD or the RH forms, plasmid was generated by removing the FVIII transgene from constructs already available in the lab and by inserting the sequence under STAB2 promoter by AgeI-SalI restriction enzymes. The LV.VEC-GFP construct used for endothelial promoter comparison was already available in our lab.[19] LVs were produced by transient co-transfection of 293T cells with third-generation packaging plasmids using the calcium phosphate method according to published protocols. LV titers were determined on 293T by qPCR as described previously.[46]

Mice

For GFP expression studies, 8- to 9-week-old C57BL/6J (The Jackson Laboratory, no. 000664) and BALB/cJ (The Jackson Laboratory, no. 000651) were injected with 5×10^8 transducing units (TU) of LV.STAB2-GFP, while LV.PGK-GFP was used as control for its ubiquitous promoter. For *in vivo* tolerance studies, 8- to 9-week-old B10.D2 mice (The Jackson Laboratory, no. 000463) were tail-vein injected with 5×10^8 TU of LV.STAB2-GFP or LV. VEC-GFP (with or without the mirTs-122.142). Mice injected with 3×10^8 TU of LV.PGK-GFP were used as controls. Ten-week-old B10.D2 and JEDI mice,[25] kindly donated by Dr Brown (Mount Sinai, NY), were used as $CD8^+$ T cells donor for *in vivo* adoptive transfer and *in vitro* co-culture experiments. The original FVIII knockout mice B6;129-*F8*^{tm1Kaz}/J (B6/129 HA)[47] were purchased from The Jackson Laboratory (no. 004424), while the C57BL/6 HA mice were kindly provided by Professor L. Naldini (HSR-TIGET). These mice were injected with 10^9 TU of LV-expressing hFVIII-BDD and hFVIII-RH forms under the control of STAB2p. All animals were kept under specific pathogen-free conditions and all the procedures were reviewed and approved by the Animal Care and Use Committee of Università del Piemonte Orientale and by the Italian Health Ministry (Authorization no. 370/2019-PR, project DB064.45, and authorization no. 183/2020-PR project DB064.48).

IF

Liver and spleen of all LV-injected mice were collected 14 days (1, 2, or 3 months) after mice injection, fixed in 4% paraformaldehyde (PFA) in PBS, equilibrated in 15% sucrose in PBS overnight followed by 48 h in 30% sucrose in PBS and embedded in optimal-temperature cutting medium (O.C.T.). Four-μm-thick cryostat sections were fixed with 4% PFA at room temperature (RT) for 5 min. Organ sections were rinsed in PBS 1×, incubated with blocking solution (0.1% Triton X-100, 1% bovine serum albumin [BSA], in PBS 1×, PBST) containing 5% goat serum (GS) for 1 h at RT in a humid chamber. Primary antibodies were prepared with PBST with 2% GS and incubated for 1 h at RT in a humid chamber. Samples were then washed 3 times with PBS- Tween 0.1% (PBS-T) and incubated in a humid dark chamber with secondary antibodies that were previously prepared with PBST and 4′-6-diamidino-2-phenylindole (nuclear staining, dilution 1:200). After 30 min, samples were washed at least 3 times with PBS 1× and mounted with Moviol (Sigma-Aldrich). Images were acquired at fluorescence microscope (Leica DM 2500) and analyzed using LASX software (Leica Application Suite X) and ImageJ software. The antibodies used are listed in Table S1. Quantification of IF colocalization areas was performed on four to six different pictures/mouse by writing a specific macro for the software ImageJ, using a value interval between 3 and 5. Graphs represent the percentage of red staining area (F4/80 or LYVE1) over the GFP-detected area. Quantification by ImageJ software of the GFP area in Figure 4N is expressed as pixels/μm^2.

Flow cytometry analysis

At the time of euthanasia, single-cell suspensions were prepared from liver after mechanical disaggregation followed by Ficoll-Paque (Sigma-Aldrich) gradient centrifugation and from spleen after red blood cell (RBC) lysis. Samples were stained with fluorochrome-labeled monoclonal antibodies (Table S1) against mouse markers. Antibody master mixes were made for each staining in FACS buffer (PBS, 2% FBS, 2 mM EDTA). Cells were washed and resuspended in each master mix and incubated for 15 min at 4°C. Samples were acquired on the Attune NxT Acoustic Focusing Cytometer (Thermo Fisher Scientific) and analyses were performed using FlowJo v10 software (BD Biosciences). A representative gating strategy for identification of $CD4^+$ and $CD8^+$ T cells (including $CD44^+$ and $PD1^+$ gates), myeloid $CD11b^+Gr1^-$ cells, $CD11b^+Gr1^+$ granulocytes, and $CD19^+$ B cells, is shown in Figure S12. Antibodies used are listed in Table S2.

In vivo $CD8^+$ T cell adoptive transfer

Spleens were extracted from mice and maintained in cold Roswell Park Memorial Institute (RPMI) medium supplemented with 5% FBS until processing. Single-cell suspensions were obtained by mechanical disaggregation and filtration through a 40-μm cell strainer. RBCs from spleen were lysed by adding ammonium chloride solution for 5 min. Total splenocytes were centrifuged and resuspended in MACS buffer (PBS 0.5% BSA, 2 mM EDTA). B10.D2 or JEDI $CD8^+$ T cell isolation was performed using a $CD8a^+$ T Cell Isolation Kit (Miltenyi Biotec) following the manufacturer's protocol. In brief, resuspended splenocytes were stained with a cocktail of biotin-conjugated monoclonal

antibodies (CD4, CD19, CD11b, CD11c, CD45R [B220], CD49b [DX5], CD105, MHC class II, Ter-119, TCRγ/δ) and loaded on a magnetic column after labeling with anti-biotin microbeads. The population of interest was obtained through negative selection, and the purity of $CD8^+$ T cells was checked by flow cytometry. Only fractions with more than 90% of $CD8^+$ cells were used for the *in vivo* transfer. Ten days after the LV administration, $1.5–2 \times 10^6$ $CD8^+$ T cells were intravenously (i.v.) injected into B10.D2 mice; 4 days later the mice were killed and liver and spleen were collected for IF and flow cytometry analysis.

Macrophage isolation and co-culture with splenocytes

Peritoneal macrophages were isolated from B10.D2 mice through PBS peritoneal washing in 10 mL and their number was evaluated by FACS using CD19 and F4/80 antibody (Figures S13A and S13B). A total of $1–2 \times 10^5$ macrophages were plated on a p48 well plate and cultured in DMEM supplemented with 10% FBS; after 24 h they were transduced with LV.PGK-GFP at multiplicity of infection 7 and allowed to grow for 3 days, until GFP expression was evident on the microscope (Figures S13C and S13D). Untransduced macrophages were used as controls. At day 4, 5×10^5 total splenocytes/well were added and co-cultured for 3 days with the macrophages in RPMI with 10% FBS; the splenocytes were harvested from B10.D2 mice injected 14 days before the killing with LV.STAB2-GFP or LV.PGK-GFP. JEDI splenocytes were used as positive control. At the end of the co-culture, supernatants were collected and assessed for Granzyme B concentration, while the number and phenotype of $CD8^+$ T cells were evaluated by flow cytometry. Macrophage viability was tested by MTT assay.

Mouse Granzyme B detection

Concentration of mouse Granzyme B was measured in the collected supernatants from the macrophage and splenocyte coculture by the enzyme-linked immunosorbent assay (ELISA) according to the manufacturer's protocol (Granzyme B Mouse ELISA Kit, ThermoFisher Scientific).

MTT assay

Macrophage viability after co-culture with $CD8^+$ T cells was evaluated by the (3-(4,5-dimethylthiazol-2-yl)-2,5-diphenyltetrazolium bromide colorimetric assay (MTT, Sigma). In brief, 1:10 MTT solution (5 mg/mL in PBS) was added to complete medium for each sample and incubated for 2 h at 37°C in the dark. Formazan crystals were solved with 100 μL of dimethyl sulphoxide (Sigma) and supernatant optical density was evaluated at 570 nm using a spectrophotometer (Victor, PerkinElmer). Results are reported in graphs as percentages of cell viability vs. the corresponding control (GFP^+ transduced or GFP^- untransduced macrophages).

Detection of FVIII activity (aPTT assay) and anti-FVIII IgG antibodies (ELISA)

The presence of FVIII activity was evaluated in plasma of treated mice starting from 2 weeks after injection, as described previously.[42] The percentage of FVIII activity was quantified by one-stage aPTT using HemosIL Synthasil aPTT reagents (Instrumentation Laboratory) in a Coatron M4 coagulometer (TECO Medical Instruments). Standards for FVIII activity quantification were generated by serially diluting recombinant human BDD-FVIII (RefactoAF, Pfizer) in HA mouse plasma.

The presence of anti-FVIII IgG antibodies in plasma of LV-injected mice was evaluated by indirect ELISA on a 96-well plate coated with 0.2 μg/mL FVIII-BDD (ReFactoAF) as described previously.[19] Anti-FVIII IgG antibodies were detected using horseradish peroxidase-conjugated goat anti-mouse IgG Fc secondary antibody (Thermo Fisher Scientific). Plasma from HA mice previously immunized with LV.PGK-FVIII and reacting against FVIII was used as positive control, while pooled plasma from untreated HA mice served as negative control.

In vivo Treg depletion

To obtain Treg depletion, HA mice were treated i.v. with 300 μg of α-CD25 antibodies (clone PC61, Bio X Cell) either 1 or 14 weeks after LV injection.

Tail clip challenge

Tail clip assay was performed as described previously.[48] Mice tails (2.5–3 mm in diameter) were cut after anesthetization of the animals and immersed in saline solution at 37°C. Blood was allowed to flow for a maximum of 10 min and tails were then removed and cauterized. Blood loss was evaluated by reading 570 nm absorbance on Victor X (PerkinElmer) after sample centrifugation and RBC lysis.

Statistical analyses

For statistical analysis the program GraphPad Prism10 was used. A Mann-Whitney U test was run to compare the percentage of IF colocalization. One-way analysis of variance (ANOVA) with post-hoc Tukey test was performed to compare ten groups. Two-way ANOVA was used to resolve overall effects on FVIII activity or IgG level between different groups of treated mice over time; a Sidak's multiple comparison test was run for each time point. $p < 0.05$ was deemed significant, $^*p \leq 0.05$, $^{**}p \leq 0.01$, $^{***}p \leq 0.001$, $^{****}p \leq 0.0001$.

DATA AND CODE AVAILABILITY

All data associated with this study are available from the authors without any restrictions.

SUPPLEMENTAL INFORMATION

Supplemental information can be found online at https://doi.org/10.1016/j.omtn.2024.102116.

ACKNOWLEDGMENTS

The study was partially supported by Fondazione Cariplo grant no. 2018-0253 (to C.B.), by Fondazione Telethon no. GGP19201, and by Compagnia di San Paolo-Bando - Trapezio linea 1 (to A.F.). The authors would like to thank Dr Marcello Arsura for the scientific English revision.

AUTHOR CONTRIBUTIONS

C.B. and A.F. provided the conceptual framework for the study. E.B., C.B., S.M., and A.F. designed the experiments. E.B., C.B., R.A.C., V.K., R.F., and S.M. performed the experiments and analyzed the data. B.B. provided the JEDI mice and critical comments on the manuscript. E.B., C.B., and A.F. wrote the manuscript, which was critically revised by all authors.

DECLARATION OF INTERESTS

A.F., S.M., E.B., and C.B. are named inventors of the patent "Endothelial-specific promoter sequences and use thereof." Publication no. 20200165631, filed July 26, 2018, and issued May 28, 2020 (PCT/IB2018/055603).

REFERENCES

1. Horst, A.K., Neumann, K., Diehl, L., and Tiegs, G. (2016). Modulation of liver tolerance by conventional and nonconventional antigen-presenting cells and regulatory immune cells. Cell. Mol. Immunol. *13*, 277–292.
2. Carambia, A., Freund, B., Schwinge, D., Heine, M., Laschtowitz, A., Huber, S., Wraith, D.C., Korn, T., Schramm, C., Lohse, A.W., et al. (2014). TGF-β-dependent induction of CD4+CD25+Foxp3+ Tregs by liver sinusoidal endothelial cells. J. Hepatol. *61*, 594–599.
3. El-Maarri, O., Jamil, M.A., and Oldenburg, J. (2020). Molecular Profiling of Liver Sinusoidal Endothelial Cells in Comparison to Hepatocytes: Reflection on Which Cell Type Should Be the Target for Gene Therapy. Hämostaseologie *40*, S26–S31.
4. Gottwick, C., Carambia, A., and Herkel, J. (2022). Harnessing the liver to induce antigen-specific immune tolerance. Semin. Immunopathol. *44*, 475–484.
5. Crispe, I.N. (2011). Liver antigen-presenting cells. J. Hepatol. *54*, 357–365.
6. Paez-Cortez, J., Montano, R., Iacomini, J., and Cardier, J. (2008). Liver Sinusoidal Endothelial Cells as Possible Vehicles for Gene Therapy: A Comparison Between Plasmid-Based and Lentiviral Gene Transfer Techniques. Endothelium *15*, 165–173.
7. Carambia, A., Freund, B., Schwinge, D., Bruns, O.T., Salmen, S.C., Ittrich, H., Reimer, R., Heine, M., Huber, S., Waurisch, C., et al. (2015). Nanoparticle-based autoantigen delivery to Treg-inducing liver sinusoidal endothelial cells enables control of autoimmunity in mice. J. Hepatol. *62*, 1349–1356.
8. Bolton-Maggs, P.H.B., and Pasi, K.J. (2003). Haemophilias A and B. Lancet *361*, 1801–1809.
9. Peyvandi, F., and Garagiola, I. (2019). Clinical advances in gene therapy updates on clinical trials of gene therapy in haemophilia. Haemophilia *25*, 738–746.
10. Samelson-Jones, B.J., and George, L.A. (2023). Adeno-associated Virus Gene Therapy for Hemophilia. Annu. Rev. Med. *74*, 231–247.
11. George, L.A., Monahan, P.E., Eyster, M.E., Sullivan, S.K., Ragni, M.V., Croteau, S.E., Rasko, J.E.J., Recht, M., Samelson-Jones, B.J., MacDougall, A., et al. (2021). Multiyear Factor VIII Expression after AAV Gene Transfer for Hemophilia. N. Engl. J. Med. *385*, 1961–1973.
12. Pasi, K.J., Rangarajan, S., Mitchell, N., Lester, W., Symington, E., Madan, B., Laffan, M., Russell, C.B., Li, M., Pierce, G.F., and Wong, W.Y. (2020). Multiyear Follow-up of AAV5-hFVIII-SQ Gene Therapy for Hemophilia. N. Engl. J. Med. *382*, 29–40.
13. Mahlangu, J., Kaczmarek, R., von Drygalski, A., Madan, B., , et al.von, Shapiro, S., Chou, S.-C., Ozelo, M.C., Kenet, G., Peyvandi, F., et al. (2023). Two-Year Outcomes of Valoctocogene Roxaparvovec Therapy for Hemophilia. N. Engl. J. Med. *388*, 694–705.
14. Milone, M.C., and O'Doherty, U. (2018). Clinical use of lentiviral vectors. Leukemia *32*, 1529–1541.
15. Do, H., Healey, J.F., Waller, E.K., and Lollar, P. (1999). Expression of Factor VIII by Murine Liver Sinusoidal Endothelial Cells. J. Biol. Chem. *274*, 19587–19592.
16. Kumaran, V., Benten, D., Follenzi, A., Joseph, B., Sarkar, R., and Gupta, S. (2005). Transplantation of endothelial cells corrects the phenotype in hemophilia A mice. J. Thromb. Haemost. *3*, 2022–2031.
17. Sørensen, K.K., Simon-Santamaria, J., McCuskey, R.S., and Smedsrød, B. (2015). Liver Sinusoidal Endothelial Cells. Compr. Physiol. *5*, 1751–1774.
18. Zanolini, D., Merlin, S., Feola, M., Ranaldo, G., Amoruso, A., Gaidano, G., Zaffaroni, M., Ferrero, A., Brunelleschi, S., Valente, G., et al. (2015). Extrahepatic sources of factor VIII potentially contribute to the coagulation cascade correcting the bleeding phenotype of mice with hemophilia A. Haematologica *100*, 881–892.
19. Merlin, S., Cannizzo, E.S., Borroni, E., Bruscaggin, V., Schinco, P., Tulalamba, W., Chuah, M.K., Arruda, V.R., VandenDriessche, T., Prat, M., et al. (2017). A Novel Platform for Immune Tolerance Induction in Hemophilia A Mice. Mol. Ther. *25*, 1815–1830.
20. Bhandari, S., Larsen, A.K., McCourt, P., Smedsrød, B., and Sørensen, K.K. (2021). The Scavenger Function of Liver Sinusoidal Endothelial Cells in Health and Disease. Front. Physiol. *12*, 757469.
21. Olsavszky, V., Sticht, C., Schmid, C.D., Winkler, M., Wohlfeil, S.A., Olsavszky, A., Schledzewski, K., Géraud, C., Goerdt, S., Leibing, T., and Koch, P.S. (2021). Exploring the transcriptomic network of multi-ligand scavenger receptor Stabilin-1- and Stabilin-2-deficient liver sinusoidal endothelial cells. Gene *768*, 145284.
22. Swystun, L.L., Lai, J.D., Notley, C., Georgescu, I., Paine, A.S., Mewburn, J., Nesbitt, K., Schledzewski, K., Géraud, C., Kzhyshkowska, J., et al. (2018). The endothelial cell receptor stabilin-2 regulates VWF-FVIII complex half-life and immunogenicity. J. Clin. Invest. *128*, 4057–4073.
23. Follenzi, A., Battaglia, M., Lombardo, A., Annoni, A., Roncarolo, M.G., and Naldini, L. (2004). Targeting lentiviral vector expression to hepatocytes limits transgene-specific immune response and establishes long-term expression of human antihemophilic factor IX in mice. Blood *103*, 3700–3709.
24. Chen, Y., Pikkarainen, T., Elomaa, O., Soininen, R., Kodama, T., Kraal, G., and Tryggvason, K. (2005). Defective Microarchitecture of the Spleen Marginal Zone and Impaired Response to a Thymus-Independent Type 2 Antigen in Mice Lacking Scavenger Receptors MARCO and SR-A. J. Immunol. *175*, 8173–8180.
25. Agudo, J., Ruzo, A., Park, E.S., Sweeney, R., Kana, V., Wu, M., Zhao, Y., Egli, D., Merad, M., and Brown, B.D. (2015). GFP-specific CD8 T cells enable targeted cell depletion and visualization of T-cell interactions. Nat. Biotechnol. *33*, 1287–1292.
26. Keir, M.E., Butte, M.J., Freeman, G.J., and Sharpe, A.H. (2008). PD-1 and Its Ligands in Tolerance and Immunity. Annu. Rev. Immunol. *26*, 677–704.
27. Knolle, P.A., and Wohlleber, D. (2016). Immunological functions of liver sinusoidal endothelial cells. Cell. Mol. Immunol. *13*, 347–353.
28. Mates, J.M., Yao, Z., Cheplowitz, A.M., Suer, O., Phillips, G.S., Kwiek, J.J., Rajaram, M.V.S., Kim, J., Robinson, J.M., Ganesan, L.P., and Anderson, C.L. (2017). Mouse Liver Sinusoidal Endothelium Eliminates HIV-Like Particles from Blood at a Rate of 100 Million per Minute by a Second-Order Kinetic Process. Front. Immunol. *8*, 35.
29. Limmer, A., Ohl, J., Kurts, C., Ljunggren, H.G., Reiss, Y., Groettrup, M., Momburg, F., Arnold, B., and Knolle, P.A. (2000). Efficient presentation of exogenous antigen by liver endothelial cells to CD8+ T cells results in antigen-specific T-cell tolerance. Nat. Med. *6*, 1348–1354.
30. Schurich, A., Berg, M., Stabenow, D., Böttcher, J., Kern, M., Schild, H.-J., Kurts, C., Schuette, V., Burgdorf, S., Diehl, L., et al. (2010). Dynamic regulation of CD8 T cell tolerance induction by liver sinusoidal endothelial cells. J. Immunol. *184*, 4107–4114.
31. Böttcher, J.P., Schanz, O., Garbers, C., Zaremba, A., Hegenbarth, S., Kurts, C., Beyer, M., Schultze, J.L., Kastenmüller, W., Rose-John, S., and Knolle, P.A. (2014). IL-6 trans-Signaling-Dependent Rapid Development of Cytotoxic CD8+ T Cell Function. Cell Rep. *8*, 1318–1327.
32. Dudek, M., Lohr, K., Donakonda, S., Baumann, T., Lüdemann, M., Hegenbarth, S., Dübbel, L., Eberhagen, C., Michailidou, S., Yassin, A., et al. (2022). IL-6-induced FOXO1 activity determines the dynamics of metabolism in CD8 T cells cross-primed by liver sinusoidal endothelial cells. Cell Rep. *38*, 110389.
33. Knolle, P.A., Schmitt, E., Jin, S., Germann, T., Duchmann, R., Hegenbarth, S., Gerken, G., and Lohse, A.W. (1999). Induction of cytokine production in naive CD4+ T cells by antigen-presenting murine liver sinusoidal endothelial cells but failure to induce differentiation toward Th1 cells. Gastroenterology *116*, 1428–1440.
34. Carambia, A., Frenzel, C., Bruns, O.T., Schwinge, D., Reimer, R., Hohenberg, H., Huber, S., Tiegs, G., Schramm, C., Lohse, A.W., and Herkel, J. (2013). Inhibition of

inflammatory CD4 T cell activity by murine liver sinusoidal endothelial cells. J. Hepatol. *58*, 112–118.

35. Dingle, A.M., Yap, K.K., Gerrand, Y.-W., Taylor, C.J., Keramidaris, E., Lokmic, Z., Kong, A.M., Peters, H.L., Morrison, W.A., and Mitchell, G.M. (2018). Characterization of isolated liver sinusoidal endothelial cells for liver bioengineering. Angiogenesis *21*, 581–597.

36. Annoni, A., Gregori, S., Naldini, L., and Cantore, A. (2019). Modulation of immune responses in lentiviral vector-mediated gene transfer. Cell. Immunol. *342*, 103802.

37. Falkowski, M., Schledzewski, K., Hansen, B., and Goerdt, S. (2003). Expression of stabilin-2, a novel fasciclin-like hyaluronan receptor protein, in murine sinusoidal endothelia, avascular tissues, and at solid/liquid interfaces. Histochem. Cell Biol. *120*, 361–369.

38. Kaczmarek, J., Homsi, Y., van Üüm, J., Metzger, C., Knolle, P.A., Kolanus, W., Lang, T., and Diehl, L. (2014). Liver Sinusoidal Endothelial Cell-Mediated CD8 T Cell Priming Depends on Co-Inhibitory Signal Integration over Time. PLoS One *9*, e99574.

39. Diehl, L., Schurich, A., Grochtmann, R., Hegenbarth, S., Chen, L., and Knolle, P.A. (2008). Tolerogenic maturation of liver sinusoidal endothelial cells promotes B7-homolog 1-dependent CD8+ T cell tolerance. Hepatology *47*, 296–305.

40. Garrod, K.R., Moreau, H.D., Garcia, Z., Lemaître, F., Bouvier, I., Albert, M.L., and Bousso, P. (2012). Dissecting T Cell Contraction In Vivo Using a Genetically Encoded Reporter of Apoptosis. Cell Rep. *2*, 1438–1447.

41. Collins, P.W., Blanchette, V.S., Fischer, K., Björkman, S., Oh, M., Fritsch, S., Schroth, P., Spotts, G., Astermark, J., and Ewenstein, B.; rAHF-PFM Study Group (2009). Break-through bleeding in relation to predicted factor VIII levels in patients receiving prophylactic treatment for severe hemophilia A. J. Thromb. Haemost. *7*, 413–420.

42. Merlin, S., Famà, R., Borroni, E., Zanolini, D., Bruscaggin, V., Zucchelli, S., and Follenzi, A. (2019). FVIII expression by its native promoter sustains long-term correction avoiding immune response in hemophilic mice. Blood Adv. *3*, 825–838.

43. Scott, D.W., and Pratt, K.P. (2019). Factor VIII: Perspectives on Immunogenicity and Tolerogenic Strategies. Front. Immunol. *10*, 3078.

44. Curotto de Lafaille, M.A., and Lafaille, J.J. (2009). Natural and Adaptive Foxp3+ Regulatory T Cells: More of the Same or a Division of Labor? Immunity *30*, 626–635.

45. Nathwani, A.C. (2022). Gene therapy for hemophilia. Hematology *2022*, 569–578.

46. Follenzi, A., and Naldini, L. (2002). Generation of HIV-1 derived lentiviral vectors. Methods Enzym *346*, 454–465.

47. Bi, L., Lawler, A.M., Antonarakis, S.E., High, K.A., Gearhart, J.D., and Kazazian, H.H. (1995). Targeted disruption of the mouse factor VIII gene produces a model of haemophilia A. Nat. Genet. *10*, 119–121.

48. Schuettrumpf, J., Herzog, R.W., Schlachterman, A., Kaufhold, A., Stafford, D.W., and Arruda, V.R. (2005). Factor IX variants improve gene therapy efficacy for hemophilia B. Blood *105*, 2316–2323.